Available online at www.CivileJournal.org

Civil Engineering Journal

(E-ISSN: 2476-3055; ISSN: 2676-6957)

Vol. 11, No. 06, June, 2025

Stability Analysis of Dam with Asphalt Core in Static and Pseudo-Static Conditions

Denik Sri Krisnayanti [1*], Tri M. W. Sir [1], Elsy E. Hangge [1], Batara Doa Megonondo [2], Ralno R. Klau [3], Andrea Z. Galla [1]

[1] *Faculty of Science and Engineering, Nusa Cendana University, Kupang 85228, Indonesia.*

[2] *Faculty of Engineering, Brawijaya University, Malang 65145, Indonesia.*

[3] *Faculty of Teacher Training and Education, Nusa Cendana University, Kupang 85228, Indonesia.*

Received 25 December 2024; Revised 07 May 2025; Accepted 11 May 2025; Published 01 June 2025

Abstract

Manikin Dam was constructed to address the issue of raw water shortage in Kupang Regency and Kupang City. However, there were challenges due to clay materials that did not meet the required specifications. Therefore, this study aimed to use asphalt core design as an alternative by analyzing the stability of the embankment body under both static and pseudo-static conditions. To achieve the aim, the Bishop method was applied using the GeoStudio SLOPE/W application, along with manual calculations. The results showed that the safety factor (SF) at the end of construction without seismic loads met the minimum value of 1.300. Under various water level conditions (FWL, NWL, LWL), SF consistently met the minimum required value of 1.500. Furthermore, the seismic analysis considered both operational base earthquakes (OBE) with a return period of 100 years and maximum design earthquakes (MDE), which had a return period of 5,000 years. Even under OBE and MDE seismic loading conditions, SF exceeded the minimum required value. This implied that the use of an asphalt core could be considered safe in terms of preventing potential landslides under both static and pseudo-static conditions. Based on this outcome, asphalt core became a practical alternative for future dam construction, particularly in areas where clay could be scarce or unstable for technical reasons.

Keywords: Stability; Dam; Asphalt Core; Static; Pseudo-static.

1. Introduction

Water resource management is becoming an increasingly significant global challenge due to population growth and climate change. Dams serve as a primary solution to these challenges, as their presence enhances access to clean water and improves community quality of life. Dam construction plays an essential and irreplaceable role in ensuring a stable and reliable water supply by storing and regulating water flow [1]. Additionally, dams are designed to collect rainwater for use during the dry season, which is particularly beneficial in regions with low rainfall variability, such as Kupang City, where prolonged droughts are common [2]. The dry season significantly impacts both communities and the agricultural sector, leading to water shortages. Therefore, dam construction represents a strategic solution for water resource management, providing security and reliability in water supply.

The construction of the dam located in Taebenu District, Kupang Regency, is a large-scale project aimed at addressing the shortage of raw water supply in both Kupang Regency and Kupang City, with a storage capacity of

* Corresponding author: denik.krisnayanti@staf.undana.ac.id

http://dx.doi.org/10.28991/CEJ-2025-011-06-024

approximately 20.45 million m³. This dam is designed to irrigate an agricultural area of around 570 hectares, provide raw water distribution at a rate of 700 liters per second, and serve as flood control [2, 3]. Manikin Dam was conceived as a vertical zoned core dam, with asphalt designated as the impermeable zone. Asphalt was chosen as a substitute for clay due to the incompatibility of the local clay material with the embankment volume requirements and the plasticity index specifications needed for constructing the core zone. Furthermore, the decision to use asphalt was influenced by considerations of cost-effectiveness and project time constraints [4]. Asphalt, when used as the core of the dam body (Asphalt Concrete Core, ACC), is waterproof, homogeneous, flexible, and well-suited for earthquake-prone areas [5, 6]. Another advantage of using asphalt in the dam core is that construction is not affected by weather conditions [7]. In regions with high rainfall, the total construction duration for an asphalt core is shorter compared to other dam types [8]. The ductile nature of asphalt allows it to remain intact even under significant deformation within the dam body [9].

Despite the proven effectiveness of asphalt-core dams in certain applications, these structures possess numerous potential vulnerabilities that must be addressed during both the design and maintenance phases. These vulnerabilities include the effects of aging caused by intrinsic factors such as asphalt content and binder film thickness, as well as extrinsic factors like environmental exposure [10]. Permeability issues [11] and the impact of temperature variations on stability [7, 12] are also significant concerns. Given the unique properties of asphalt compared to traditional core materials such as clay or concrete, conducting stability analyses is particularly important for asphalt-core dams. Moreover, while asphalt offers various advantages, it also presents challenges to long-term stability, including the risk of hydraulic fracturing [13], especially under dynamic loads like earthquakes or fluctuations in water levels [14, 15]. Earthquakes, in particular, can dramatically alter the forces acting on the dam body, potentially compromising stability [16]. Therefore, the primary goal of stability analysis is to ensure the structural safety of the dam body, preventing potential disasters such as collapse [17].

Several studies have been conducted on the Manikin Dam, including investigations into the SCS Curve Number method in the Manikin Watershed [18], rainfall analysis in the Manikin Dam Watershed [19], and determining curve numbers in the Manikin Watershed using GIS software [20]. Another area of research has been the calculation of design flood discharge using the HSS method in the Manikin River Watershed [21]. However, there remains a lack of literature specifically addressing the stability of dam bodies constructed with asphalt core material. Thus, the primary objective of the present study is to elucidate the stability of asphalt-core dam bodies, considering the effects of seismic loads and the final construction stage. The analysis design includes an examination of the dam body's stability both without and with earthquake loads at the final construction stage, under various water levels (FWL, NWL, and LWL). It is anticipated that this study will contribute valuable insights to the existing body of research on asphalt-core dams, particularly the Manikin Dam.

Previous research on dam stability [22] has focused on the safety of the Banyu Urip Dam body constructed with clay material. Studies related to asphalt-core dams, such as [23], found that the Megech Dam in Ethiopia, featuring an asphalt core, demonstrated better stability than a clay core in both the upstream and downstream sections of the dam. In a related study, research on the asphalt core at Quxue Dam in Sichuan, China, revealed that the asphalt core exhibited flexible behavior, remained crack-free, and experienced no internal erosion in a high embankment dam [24]. An analysis by Merga Bayisa [25] compared the performance of clay-core and asphalt-core dams, concluding that asphalt-core dams achieved higher safety factors than clay cores under steady-state conditions and after construction completion. While several studies have addressed the stability of dams with asphalt cores, further research is required to investigate the stability behavior of asphalt-core dams under varying water levels and seismic loads.

An investigation by Roy et al. [26] proposed the use of ACC as an alternative to traditional clay core in embankment dam construction. The study found that ACC was particularly advantageous in regions with limited clay availability or high precipitation. Another recent study conducted by Rewtragulpaibul et al. [27] showed the feasibility and efficacy of ACC as a material for embankment construction. The investigation identified significant advantages, including accelerated implementation and improved flexibility in adapting to diverse geotechnical conditions. Additionally, analysis of the 124.5-meter Yele Dam in China by Yang et al. [28] provided a comprehensive understanding of the effectiveness of using a deep asphalt core to improve dam performance under various loading conditions, including hydrostatic pressure and seismic activity. The analytical results showed that the asphalt core maintains its stability and watertight integrity, further strengthening the application in large-scale dam engineering.

2. Material and Methods

2.1. Study Area and Data Collection

Manikin Dam was located between Kuaklalo and Bokong Village, Taebenu District, Kupang Regency, East Nusa Tenggara Province (NTT). Astronomically, the location was at coordinates 10°12'46" S and 123°43'04" E. The location of Manikin Dam in East Nusa Tenggara was shown in Figure 1. Relating to the study, secondary data included the 2017 Indonesian earthquake map, Manikin Dam technical data, dam geometry, and embankment material parameters. The technical data required included dam height, crest length, crest width, upstream and downstream slopes, and embankment volume, as well as reservoir water level elevation.

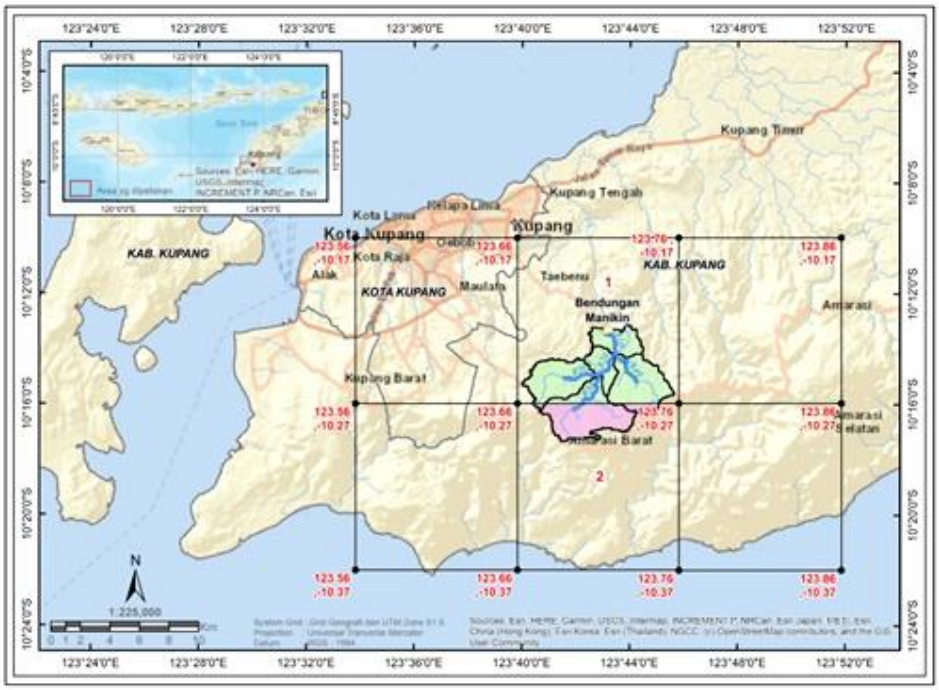

Figure 1. Manikin Dam Location

The cross-section of Manikin Dam was shown in Figure 2. The crest of the dam, situated at an elevation of +153.00 m, had upstream slope gradients of 1:3 and 1:3.5, while the downstream slope showed a ratio of 1:2. The dam structure comprised multiple zones, each with distinct functional and material characteristics. Moreover, the core zone of the dam, which functioned as an impermeable barrier, used asphalt material and was marked in red. This zone, measuring 0.7 m in width, was situated at the center of the dam body. Two filter layers were included to control water flow and maintain structural stability. The fine filter, marked in pink, was 1.5 m wide, while the coarse filter in light blue was 2 m wide.

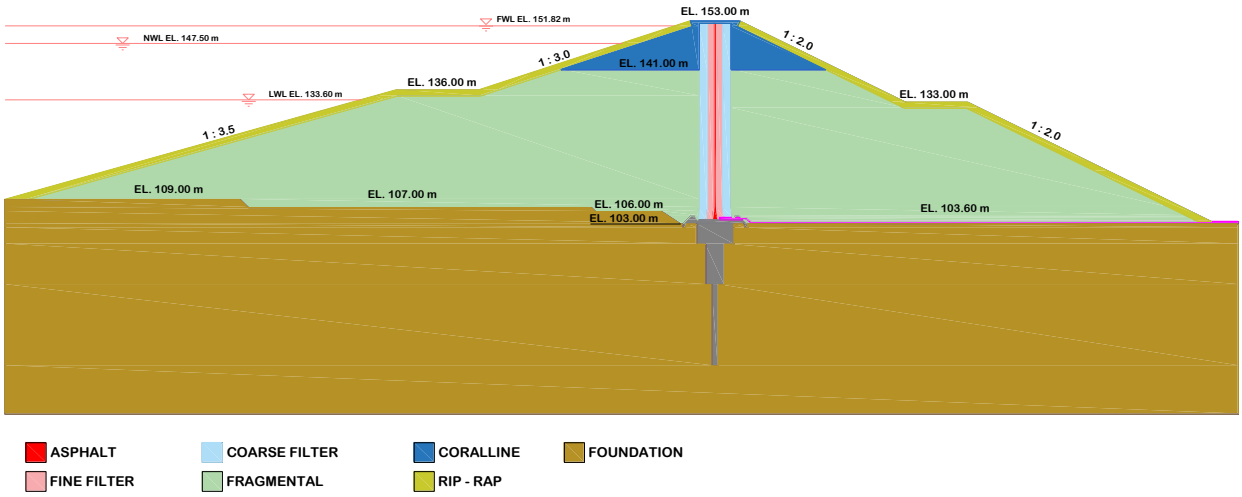

Figure 2. Manikin Dam cross-section

The random zone comprised two primary material types, namely random coralline, shown in dark blue, and random fragments, shaded in light green. The riprap zone, which served as an erosion control measure, was marked in a darker shade of yellow. Meanwhile, the foundation of the dam was shaded in brown, signifying its role as the principal structural component that undergirded the entire dam construction.

The parameters used included specific gravity in the natural state (γ) of the material, specific gravity of the material in the saturated state (γ_{sat}), cohesion (c), friction angle (ϕ), and permeability coefficient (K).

Table 1 showed that cohesion (c) in asphalt tended to be high due to its sticky nature and ability to provide resistance to shear. This high cohesion value helped reduce the risk of shear along the shear plane [29]. Although asphalt had a lower internal friction angle than granular materials such as sand or gravel in other zones, its high cohesion offset the low internal friction angle. This signified that asphalt relied more on adhesion than on friction between particles to withstand loads, making the product an effective material for maintaining the structural stability of the dam.

Table 1. Manikin Dam material parameters

Zona	Material	γ (gr/cm^3)	γ_{sat} (gr/cm^3)	c (kg/cm^2)	ϕ (°)	K (cm/s)
1	Asphalt Core	2.387	2.387	4.320	24.580	1.00E-10
2	Fine Filter	2.260	2.505	1.572	36.000	6.83E-03
3	Coarse Filter	2.250	2.768	2.571	38.670	2.87E-03
4	Fragmental	1.663	2.022	1.700	36.000	8.49E-02
5	Coraline	1.663	2.022	1.500	40.000	2.38E-02
6	Rip - Rap	1.663	2.022	0.000	45.440	2.16E-01
7	Foundation	1.783	2.121	0.047	27.670	7.18E-06

2.2. Study Framework

The framework of this study was composed of several interconnected components, as shown in Figure 3. The process of analysis started with the collection of secondary data. Furthermore, stability analysis of the dam body was conducted using the GeoStudio application and manual calculations without earthquake loads at the end of construction (SF = 1.300), flood water level (SF = 1.500), normal water level (SF = 1.500), and minimum water level (SF = 1.500). When the obtained SF met the minimum SF, the calculation proceeded with the earthquake load. Consequently, when the factor did not meet the minimum SF, modifications to the geometry had to be performed.

Modeling asphalt behavior using the Bishop method and SLOPE/W software presented several challenges, particularly due to its complex, nonlinear behavior, which included viscoelastic as well as plastic characteristics influenced by factors such as temperature, loading rate, and aging [30]. The behavior of asphalt under dynamic loads, such as seismic events, was rate-dependent. This implied that the material's response varied significantly with the velocity of loading, requiring sophisticated models to accurately capture these effects [31]. Furthermore, time-dependent changes in asphalt properties were considered during the various stages of dam construction and impounding. These alterations influenced deformation patterns as well as the total stability of the dam under both static and dynamic conditions [32, 33].

The seismic response of asphalt slabs in the dam was influenced by the angle of seismic wave incidence, which affected stress and acceleration. This required models that could accurately simulate the dynamic conditions and account for time-dependent changes in material properties [34]. Stability analysis with earthquake loads was conducted by calculating dam risk level to determine the earthquake load criteria and earthquake coefficients using the modified earthquake method at a depth of Y from the top of the dam [35]. During this analysis, the calculation for basic operational earthquake loading conditions (OBE) was performed with a minimum SF of 1.200. When the obtained SF was lesser than the minimum SF, modifications to dam geometry had to be performed. Consequently, when SF met the minimum SF, the calculation proceeded with the maximum design earthquake load (MDE) with a minimum SF of 1.000.

The deformation was expected to not exceed 50% of the maximum dam freeboard under MDE earthquake loading conditions [36]. Therefore, when the resulting SF did not meet the minimum SF, a permanent displacement analysis had to be conducted using the Makdisi-Seed method [37]. When the settlement exceeded the maximum tolerance limit, geometric modifications were required. However, when SF exceeded the maximum limit, the dam body remained stable during an earthquake.

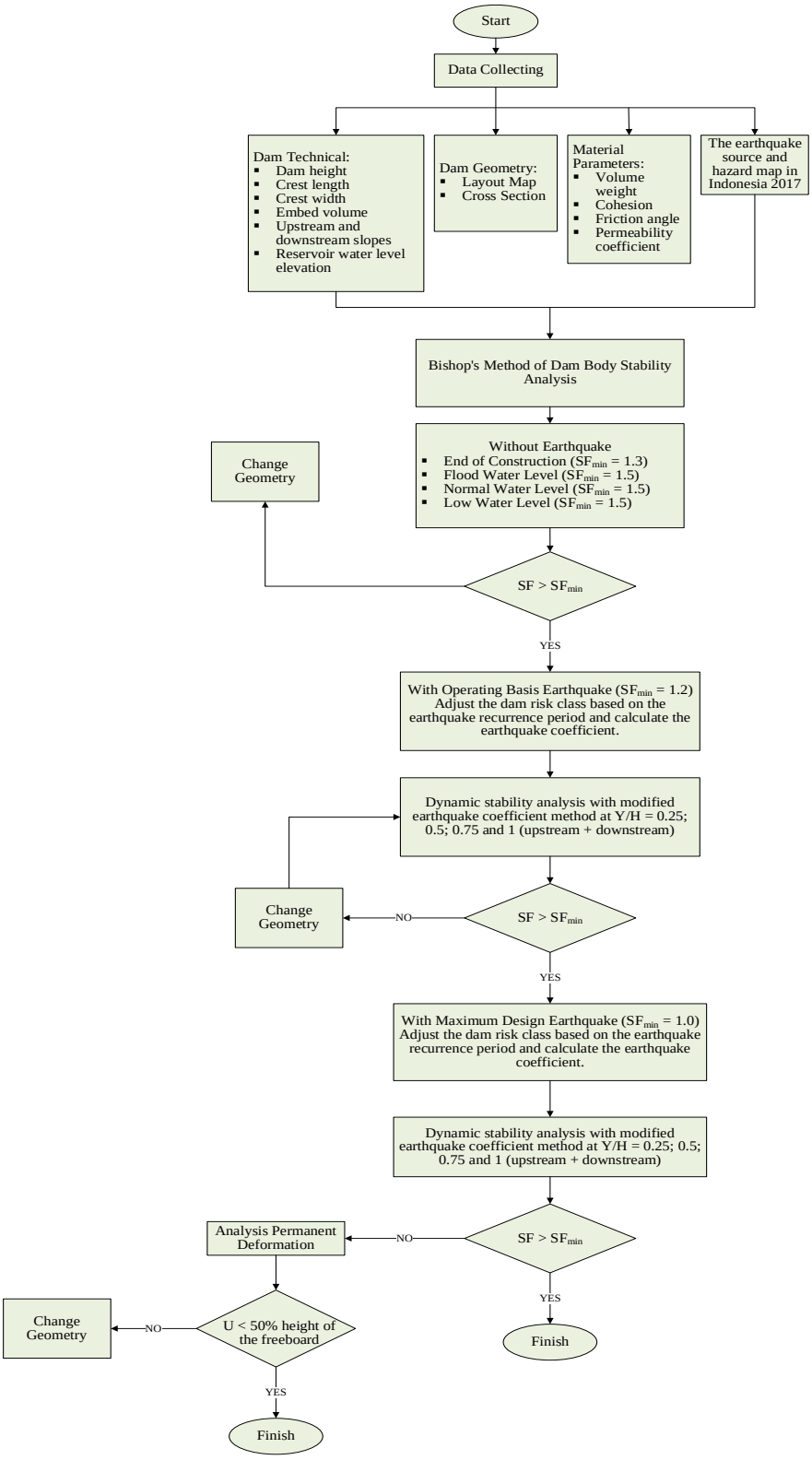

Figure 3. Study Flow Chart

2.3. Dam Stability

Stability analysis of embankment dam was conducted using two methods, namely limit equilibrium and finite element analysis. The limit equilibrium was the most practical method for analyzing dam design. On the other hand, the finite element method accounted for changes in stress and strain based on various elastic properties of materials, heterogeneity of soil mass, as well as geometric shapes. Several commonly used limit equilibrium methods were shown in Table 2. Stability results [38] were expressed in the form of SF, formulated as follows.

$$SF = \frac{\text{shear strength}}{\text{shear stress}} = \frac{S}{\tau} \quad (1)$$

Table 2. Stability Analysis Using Limit Equilibrium Method

Method	Program	Characteristic
Simplified Bishop (1955)	Mstabl, Mstab, Slope-w, Stabl-g, Sb-slope, Stablgm	Only the circular collapse plane satisfied the moment equilibrium and did not satisfy the equilibrium of horizontal as well as vertical forces.
Force Equilibrium (Lowe and Karafiat, 1960 dan US Corps of Engineers 1970)	Utexas2, Utexas3, Slope-w	All forms of collapsed planes, did not satisfy the balance of moments, satisfied the balance of horizontal and vertical forces
Janbu's Generalized Procedure (Janbu, 1968)	Stabl-g,	All forms of collapsed planes did not satisfy the balance of moments but satisfied the balance of horizontal and vertical forces.
Morgenstern and Price's, (1965)	Slope-w	The location of the lateral force could be varied in any form of collapsed plane satisfying all equilibrium conditions.
Spencer's (1967)	Mstab, Slope-w, Sb-slope, Sstab2	The location of the lateral force could be varied in any form of collapsed plane satisfying all equilibrium conditions.

The safety of the dam depended on the relationship between shear strength (s) and stress (τ). During analysis, when $s > \tau$, the dam was considered safe. Consequently, when $s < \tau$, the dam was considered to be in an unstable condition.

2.4. Dam Stability Safety Factor (SF)

Description of dam safety conditions from the results of dam stability analysis in the form of FK values [39]. The minimum SF value criteria for various dam conditions were shown in Table 3.

Table 3. Minimum SF

Condition	Minimum SF		
	Without Earthquake	OBE Earthquake	MDE Earthquake
End of Construction	1.3	1.2	1.0
Flood Water Level (FWL)	1.5		
Normal Water Level (NWL)			
Low Water Level (LWL)			

2.5. Bishop Method

Bishop method had achieved widespread recognition for its superior precision in calculating the factor of safety (SF) for slope stability. This calculation was important in ensuring the safety of asphalt core dam. The method was characterized by its ability to provide a reliable estimate of the factor of safety by accounting for the vertical equilibrium of slices. This method was advantageous because the model eliminated errors that could arise from horizontal force components [40]. Stability of Bishop method was calculated using total stress analysis and effective stress [41]. During analysis, total stress analysis was used in conditions where there was no external water load. The initial stage was to calculate the weight of slice on landslide plane using the following formula.

$$W = b \times h \times \gamma \quad (2)$$

The trial-error value was assumed for SF, and its quantity, mα, was calculated as follows.

$$m_\alpha = \cos\alpha + \frac{\sin\alpha \tan\phi}{FK} \quad (3)$$

SF was calculated using the following equation.

$$SF = \frac{\Sigma\left(\frac{cb + W\tan\phi}{m_\alpha}\right)}{\Sigma W \sin\alpha} \quad (4)$$

when there was an earthquake load, it was calculated using the following equation [42].

$$SF = \frac{\Sigma\left(\frac{cb + W\tan\phi}{m_\alpha}\right)}{\Sigma W \sin\alpha + \left(\frac{\Sigma K_h W d_i}{R}\right)} \quad (5)$$

where, SF is safety factor, c is cohesion (kN/m²), b is width of each slice (m), W is weight of slice berat pias (kN), ϕ is friction angle (°), mα is SF trial error, α is angle formed by the radius of the landslide plane (°), Kh is earthquake coefficient, di is vertical distance of the center point of the landslide plane to the center point of the slice, and R is radius of the landslide plane.

Effective stress analysis was used in the water-filled condition during the study. Due to this reason, force at the top of section and resulting moment of force about center of the circle had to be calculated [41]. The moment due to the water load was considered positive when its direction was opposite to the route of the driving moment produced by weight of landslide mass. This signified that a positive moment tended to make dam more stable. The moment during the process was calculated using the following equation.

$$M_P = P\cos\beta\, dh + P\sin\beta\, dv \quad (6)$$

with,

$$P = P_{surface} \times \frac{b}{\cos\beta} \quad (7)$$

Pore water pressure was calculated by the following equation.

$$u = h_p \times \gamma_w \quad (8)$$

SF was calculated using the following equation.

$$SF = \frac{\sum\left(\frac{cb+(W+P\cos\beta-ub)\tan\phi}{m_\alpha}\right)}{\sum W\sin\alpha-\frac{1}{R}\sum Mp} \quad (9)$$

When there was an earthquake load, it was calculated using the following equation [43].

$$SF = \frac{\sum\left(\frac{cb+(W+P\cos\beta-ub)\tan\phi}{m_\alpha}\right)}{\sum W\sin\alpha+\left(\frac{\sum K_h W d_i}{R}\right)-\left(\frac{1}{R}\sum Mp\right)} \quad (10)$$

where, Mp is moment due to surface/water load (kNm), P is surface load (kN), β is angle of inclination of the sliced surface (°), dh is horizontal moment arm (m), dv is vertical moment arm (m), u is pore water pressure (kN/m²), γ_w is specific gravity of water (kN/m³), di is vertical distance from the center point of the landslide plane to the center point of the section (m), and R is radius of landslide area.

2.6. Dam Risk Class

Dam risk factors included reservoir capacity (FRc), dam height (FRh), evacuation needs (FRe), and downstream damage (FRd) [44]. Dam risk level determined the earthquake load risk class that should be used in dam design [45], as shown in Table 4. Moreover, determination of the earthquake load class was conducted with the equation.

$$FR_{tot} = FR_c + FR_h + FR_e + FR_d \quad (11)$$

Table 4. Dam Safety Evaluation Risk Factor Criteria

Risk Factor	Value			
	Extreme	High	Moderate	Low
Capacity (10^6 m³) (FRc)	> 100 (6)	100 – 1.25 (4)	1.00 – 0.125 (2)	< 0.125 (0)
High (m) (FRh)	> 45 (6)	45 – 30 (4)	30 – 15 (2)	< 15 (0)
Evacuation Needs (number of people) (FR_e)	> 1000 (12)	1000 - 100 (8)	100 – 1 (4)	0 (0)
Downstream damage rate (FRd)	Very high (12)	High (10)	Rather High (8)	Moderate (4)	None (0)

After obtaining FR value, the next step was to determine the earthquake load criteria by selecting the risk class. The parameters for determining the risk class and earthquake load criteria were shown in Tables 5 and 6.

Table 5. Dam Risk Criteria

Total Risk Factor	Risk Class
0 – 6	I (Low)
7 – 18	II (Moderate)
19 – 30	III (High)
31 – 36	IV (Extreme)

Table 6. Earthquake Load Criteria

Risk Class with Useful Life	Requirements without damage		Requirements allowed damage without collapse	
	T (year)	Analysis Method	T (year)	Analysis Method
IV	100 – 200	Earthquake Coefficient	10000	Earthquake or Dynamic Coefficient
III	50 – 100		5000	
II	50– 100		3000	
I	50 – 100		1000	

2.7. Earthquake Load Coefficient

Earthquake load coefficient was determined by the corrected maximum earthquake acceleration value method (peak ground acceleration, PGA). The equation for finding the basic earthquake coefficient (Kh) was as follows.

$$K_h = \frac{PGA_M}{g} \quad (12)$$

$$PGA_M = S_{PGA} \times F_{PGA} \quad (13)$$

$$K_o = \alpha_2 \times K_h \quad (14)$$

where, PGA_M is maximum peak ground acceleration, K_h is basic earthquake coefficient, S_{PGA} is basic shock acceleration (cm/s²), F_{PGA} is amplification factor, g is gravitational acceleration (980.665 cm/s²), K_o is corrected design earthquake coefficient on the ground surface, and α_2 is correction for the influence of the type of structure, for embankment dam = 0.5.

For stability analysis purposes, the review was conducted at depths of Y = 0.25H, 0.50H, 0.75H, and H, where H was the height of dam [46] with the following equation:

For $0 < Y/H \leq 0.4$

$$K_o = \alpha_2 \times K_h \quad (15)$$

For $0.4 < Y/H \leqslant 1.0$

$$K = K_o \times \left(2.0 - 0.60 \times \left(\frac{Y}{H}\right)\right) \quad (16)$$

where, PGA_M is maximum peak ground acceleration, K_h is basic earthquake coefficient, S_{PGA} is basic shock acceleration (cm/s²), F_{PGA} is amplification factor, g is gravitational acceleration (980.665 cm/s²), K_o is corrected design earthquake coefficient on the ground surface, α_2 is correction for the influence of the type of structure, for embankment dam = 0.5.

3. Results and Discussion

3.1. Dam Risk Level

Table 7 calculated the risk level of Manikin Dam, which had a total risk factor of 30. Referring to Table 5, dam risk class for Manikin Dam was classified as Class III (high). The earthquake load criteria for dam design, according to Table 6, for the Operating Basis Earthquake (OBE) used a 100-year return period while MDE used a 5000-year return period.

Table 7. Manikin Dam Risk Class

Risk Factors	Quantity	Value
Capacity (10^6 m³) (FRc)	20.45	4
High (m) (FRh)	50	6
Evacuation Needs (number of people) (FRe)	100 – 1000	8
Downstream damage rate (FRd)	Very high	12
Total Risk Factors (FR_{tot})		**30**

3.2. Earthquake Load Coefficient

Earthquake load coefficient was calculated by obtaining the earthquake acceleration in bedrock (SPGA) from 2017 Indonesian earthquake map. Table 8 showed the earthquake load coefficient for OBE with a return period of 100 years and MDE with a return period of 5000 years.

Table 8. Recapitulation of Earthquake Coefficients

Return Period (Years)	S_{PGA}	F_{PGA}	PGA_M	K_o	K_h	K at Y/H			
						0.25	0.50	0.75	1.00
100 (OBE)	0.175	1.200	0.210	0.105	0.210	0.214	0.179	0.163	0.147
5000 (MDE)	0.550	1.000	0.550	0.275	0.550	0.560	0.468	0.426	0.385

Table 8 showed the horizontal earthquake coefficient (K_h) for OBE as 0.210, signifying that twenty-one percent of the weight of dam structure acted as a horizontal force pushing dam body. The horizontal earthquake coefficient for MDE was 0.550, higher compared to OBE, signifying that a greater horizontal force was borne by stability of dam structure. This stressed the importance of considering greater earthquake intensity in dam planning and design to ensure the structure could withstand horizontal loads. The earthquake coefficient for a ratio of 0.25 Y/H was higher compared to ratio of 1.00 Y/H, showing that higher locations experienced greater earthquake acceleration.

3.3. Dam body Stability without Earthquake

Stability of dam body in the absence of an earthquake was crucial to ensuring its safety and preventing potential disasters. This calculation considered various factors, such as materials, dam geometry, and water pressure, to evaluate the ability of the structure to withstand forces as well as remain stable throughout operational period. Stability assessment for Manikin Dam body was conducted under four conditions, and the calculations, performed without earthquake loads, provided valuable understanding into its resilience.

The results of Slope/W calculation in Geostudio application in Figure 4, and the manual calculation in Table 9, showed that the factors of safety in the upstream as well as downstream sections met the minimum SF for each condition. The outcome was observed that the factor of safety in the upstream section was greater compared to downstream section. This was due to the upstream slope being calmer than downstream. The factor of safety in downstream section of dam body after construction was greater compared to water-filled condition (normal, flood, and minimum water levels). After construction, dam was in a dry condition, and its effective weight was still lighter compared to water-filled condition. However, the factor of safety in the upstream section showed that the SF in the empty (end-of-construction) upstream section was lower compared to filled condition. This was due to the parameters of asphalt material, which had similar values in dry and saturated volumetric weight.

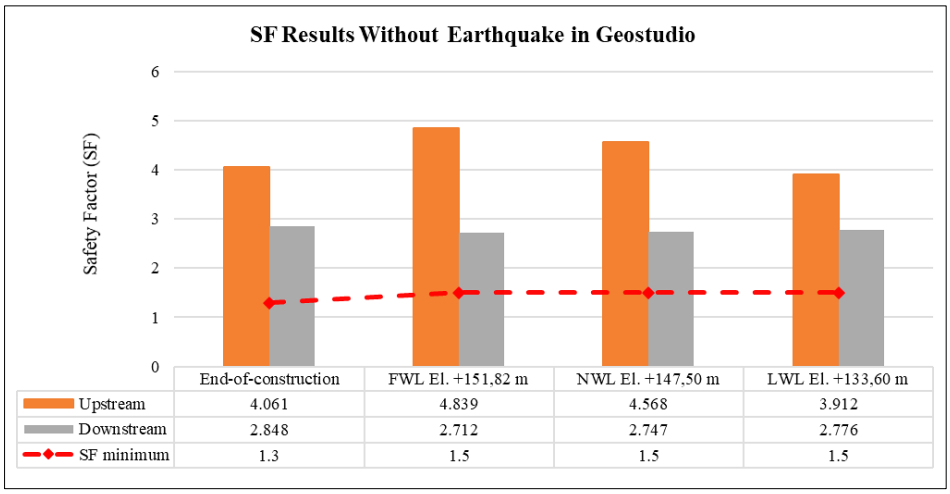

Figure 4. Dam Body SF result without earthquake in Geostudio Application

Table 9. Dam Body SF Manual Calculation without Earthquake

Condition	SF Minimum	SF Bishop	
		Upstream	Downstream
End-of-construction	1.300	4.061	2.855
Flood water level (FWL) El. +151.82 m	1.500	4.777	2.729
Normal water level (NWL) El. +147.50 m	1.500	4.549	2.756
Minimum water level (LWL) El. +133.60 m	1.500	3.686	2.790

3.4. Stability of Dam Body with Operating Basis Earthquake (OBE)

Calculations under conditions without earthquakes in upstream and downstream sections met the minimum SF, ensuring safety. Consequently, the calculation proceeded with loading OBE with a 100-year return period. Figures 5 and 6 presented Geostudio calculation, while Table 10 showed the manual calculation. SF results for upstream section of dam body were shown in Figure 5, while Figure 6 presented SF results for downstream section in Slope/W Geostudio application. These results showed that all analysis conditions met minimum SF of 1.200. The outcome was further signified that SF in condition devoid of water (end-of-construction) exceeded that of water-filled state (NWL, FWL, LWL). In the empty configuration, dam body experienced a lack of hydrostatic pressure due to the absence of water, leading to material saturation. The process during analysis showed that pore water pressure was nonexistent. However, dam body was subjected to earthquake loads, which acted upon its mass in the absence of water. When dam was filled with water, it experienced both earthquake loads and hydrostatic pressure, with the latter increasing as water depth increased. In addition, uplift pressure reduced the effective weight of the dam.

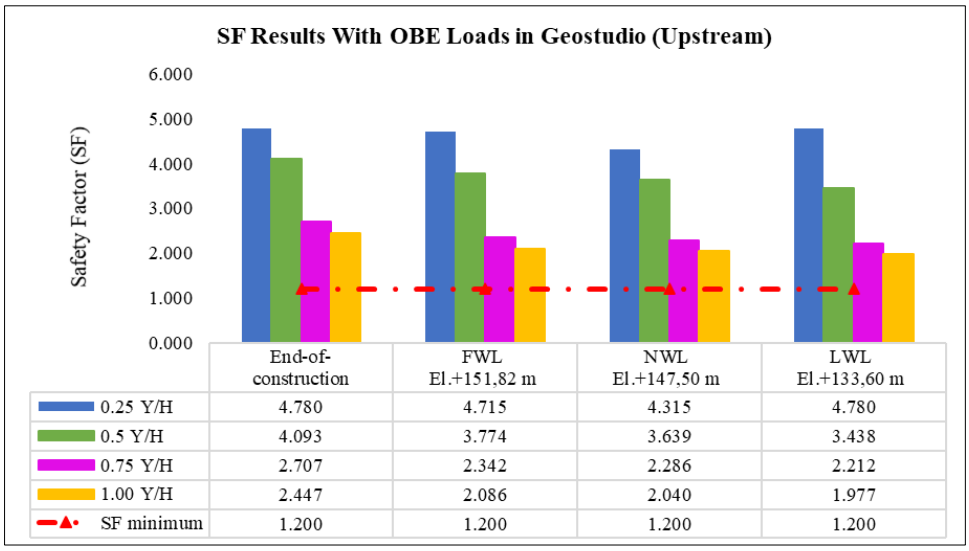

	End-of-construction	FWL El.+151,82 m	NWL El.+147,50 m	LWL El.+133,60 m
0.25 Y/H	4.780	4.715	4.315	4.780
0.5 Y/H	4.093	3.774	3.639	3.438
0.75 Y/H	2.707	2.342	2.286	2.212
1.00 Y/H	2.447	2.086	2.040	1.977
SF minimum	1.200	1.200	1.200	1.200

Figure 5. Upstream Dam Body SF result with OBE loads in Geostudio Application

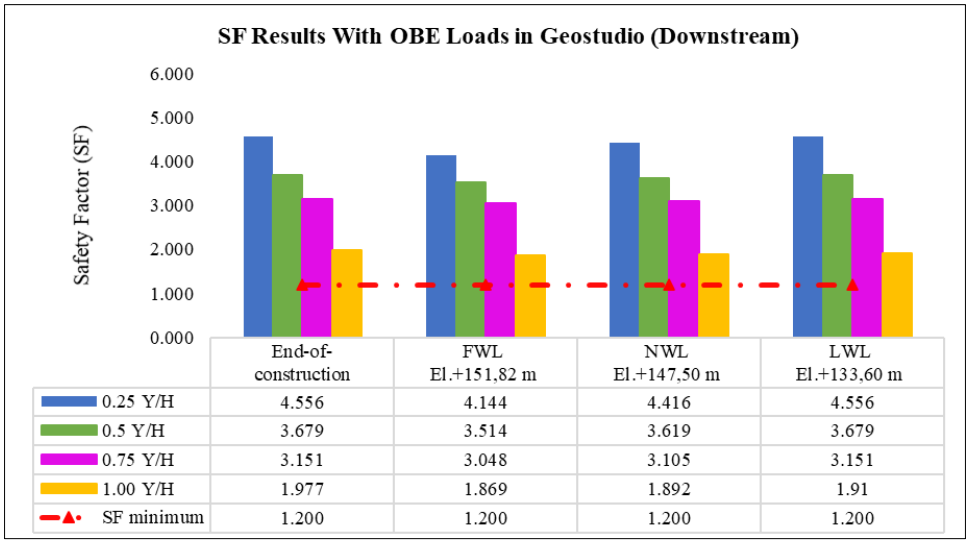

	End-of-construction	FWL El.+151,82 m	NWL El.+147,50 m	LWL El.+133,60 m
0.25 Y/H	4.556	4.144	4.416	4.556
0.5 Y/H	3.679	3.514	3.619	3.679
0.75 Y/H	3.151	3.048	3.105	3.151
1.00 Y/H	1.977	1.869	1.892	1.91
SF minimum	1.200	1.200	1.200	1.200

Figure 6. Downstream Dam Body SF result with OBE loads in Geostudio Application

Table 10 showed that the GeoStudio and manual calculation results met the minimum SF. Therefore, the dam was considered safe from landslides during an OBE. SF with an earthquake was lower than that without an earthquake due to the additional dynamic load dam had to support. During the process, OBE exerted a comparatively negligible influence on SF. This implied that the dam could withstand minor seismic events without a considerable compromise in safety.

Table 10. Dam Body SF Manual Calculations with Operating Basis Earthquake

Condition		SF Minimum	OBE (100 th)			
			0.25 Y/H	0.50 Y/H	0.75 Y/H	1.00 Y/H
			K = 0.214	K = 0.179	K = 0.163	K = 0.147
End-of-construction	US	1.200	4.778	4.096	2.710	2.448
	DS	1.200	4.546	3.674	3.154	1.990
Flood water level (FWL) El.+151.82 m	US	1.200	4.872	3.714	2.342	2.018
	DS	1.200	4.146	3.520	3.048	1.953
Normal water level (NWL) El. +147.50 m	US	1.200	4.462	3.680	2.252	2.069
	DS	1.200	4.434	3.717	3.104	1.977
Low water level (LWL) El. +133.60 m	US	1.200	4.778	3.416	2.231	1.990
	DS	1.200	4.707	3.811	3.152	1.929

3.5. Stability of Dam Body with MDE

Stability during an MDE earthquake was essential, as it could impose maximum dynamic loads on the structure. This analysis aimed to identify the impact of MDE earthquakes on dam stability and assess the mitigation measures needed to ensure dam safety. Figures 7 and 8 presented GeoStudio calculations, and Table 11 showed the manual calculations.

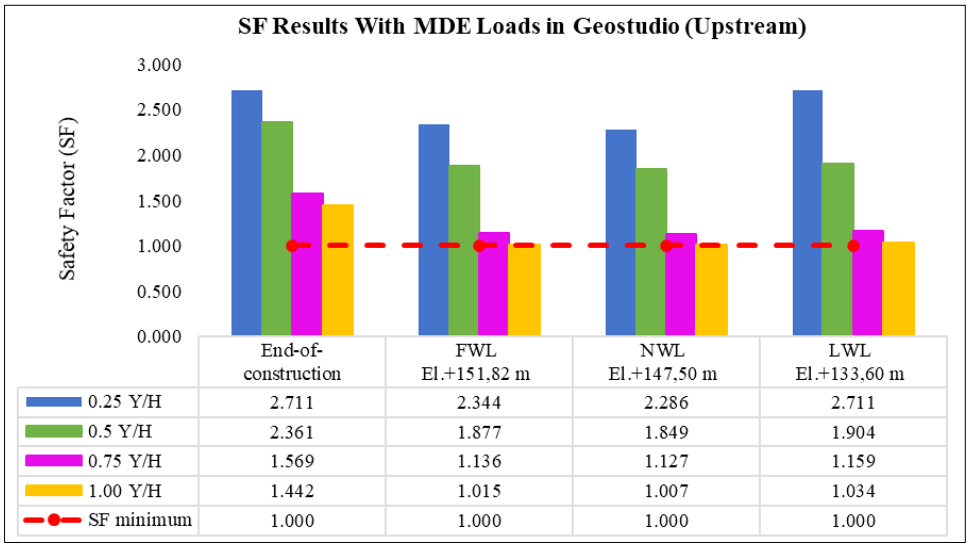

Figure 7. Upstream Dam Body SF result with MDE loads in Geostudio Application

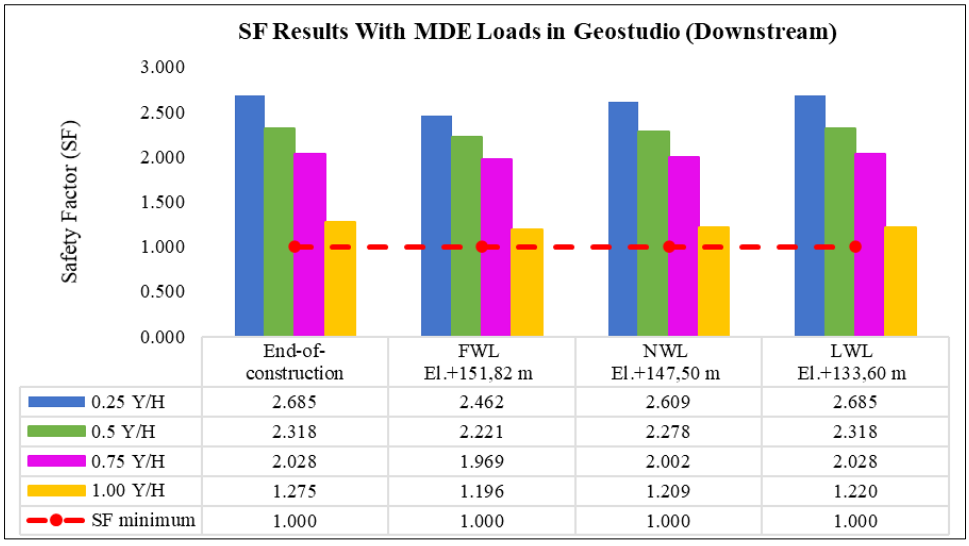

Figure 8. Downstream Dam Body SF result with MDE loads in Geostudio Application

Table 11. Dam Body SF Manual Calculations with MDE

Condition		SF Minimum	MDE (5000 th)			
			0.25 Y/H	0.50 Y/H	0.75 Y/H	1.00 Y/H
			K = 0.560	K = 0.468	K = 0.426	K = 0.385
End-of-construction	US	1.000	2.709	2.363	1.569	1.443
	DS	1.000	2.685	2.321	2.037	1.296
Flood water level (FWL) El.+151.82 m	US	1.000	2.397	1.877	1.135	1.004
	DS	1.000	2.459	2.220	1.967	1.201
Normal water level (NWL) El.+147.50 m	US	1.000	2.242	1.857	1.110	1.014
	DS	1.000	2.610	2.328	2.027	1.285
Minimum water level (LWL) El.+133.60 m	US	1.000	2.709	1.906	1.163	1.037
	DS	1.000	2.684	2.377	2.027	1.245

The calculation results indicated that the safety factor (SF) for the stability of the dam body, when analyzed under Maximum Design Earthquake (MDE) conditions, met the minimum SF requirements set by the design standards. This demonstrated that the dam possessed adequate stability to withstand the dynamic loads generated by an MDE earthquake. In other words, the dam structure was capable of safely enduring the most severe seismic conditions specified by safety criteria. Although the SF met the minimum standards, it remains essential to monitor and evaluate the dam's condition periodically.

In the context of extreme hydrological conditions, such as prolonged droughts or severe flooding, concerns have been raised regarding the safety and stability of asphalt concrete core (ACC) dams. Challenges in these situations include increased hydraulic pressure and potential issues with structural integrity during extreme flood events. Continuous monitoring and the development of predictive models are crucial for assessing the dam's response to extreme conditions and for enabling timely interventions. A comprehensive approach, incorporating both structural modifications and non-structural measures, is essential to enhance the dam's resilience against extreme hydrological events. Moreover, non-structural measures involve effective water management and emergency planning [47].

Recognizing the significant impact of thermal sensitivity on dam stability is also crucial, especially concerning asphalt materials. Elevated temperatures can cause asphalt to soften, reducing its structural stability, while lower temperatures may lead to stiffening and brittleness, increasing the risk of cracking [48, 49]. Such changes in material properties can result in structural deformation, increased seepage, and a decrease in the SF of the dam. Mitigating these impacts involves implementing asphalt stabilization techniques, such as incorporating mineral fillers and establishing a transition zone comprising fine and coarse filters to absorb thermal stresses. Furthermore, precise regulation of compaction temperature during the construction phase is vital to ensure optimal performance of asphalt as a core material. These measures are critical to maintaining the stability and safety of the dam.

4. Conclusion

In conclusion, this study evaluated the stability of an asphalt-core dam under various operating conditions, encompassing both static and earthquake-induced loads. The analysis demonstrated that the dam's safety factor (SF) satisfied the minimum required values in all examined scenarios. At the end-of-construction phase, the dam remained within the designated safety parameters, even when subjected to earthquake events such as the Operating Basis Earthquake (OBE) and the Maximum Design Earthquake (MDE). Throughout this study, the SF values obtained from the analyses indicated that the dam structure possessed sufficient resilience to withstand both dynamic and static loads during the initial operational stages. Even under extreme conditions, such as when the water level reached the Flood Water Level (FWL), the factors of safety consistently met the minimum requirements across all earthquake scenarios. This outcome signifies that the dam's design adequately accounted for the increased hydrostatic pressure associated with rising water levels during flood events, thereby ensuring structural integrity.

Under normal water level conditions, the analysis confirmed that the dam maintained its stability and fulfilled the minimum safety factor requirements. This stability reflects the dam's adaptability to routine operational demands, effectively mitigating the risk of structural failure. Furthermore, the dam demonstrated sufficient capacity to maintain the required safety factor under minimum water level conditions, both in the absence of seismic events and under earthquake conditions such as OBE and MDE. Consequently, significant fluctuations in water levels did not compromise the overall stability of the dam. The findings of this study confirm that the design of the asphalt-core dam meets the minimum safety requirements under diverse load conditions and varying water levels. Although the analyses indicate compliance with established safety standards, periodic monitoring and evaluation remain essential to ensure the dam's optimal performance throughout its intended service life.

5. Declarations

5.1. Author Contributions

Conceptualization, D.S.K. and A.Z.G.; methodology, D.S.K. and A.Z.G.; software, T.M.W.S.; validation, D.S.K., T.M.W.S., and A.Z.G.; formal analysis, D.S.K. and A.Z.G.; investigation, D.S.K., T.M.W.S., and A.Z.G.; resources, A.Z.G.; data curation, D.S.K. and A.Z.G.; writing—original draft preparation, D.S.K. and A.Z.G.; writing—review and editing, D.S.K., A.Z.G., and T.M.W.S.; visualization, D.S.K., B.D.M., and R.R.K.; supervision, D.S.K. and T.M.W.S.; project administration, D.S.K., B.D.M., and R.R.K. All authors have read and agreed to the published version of the manuscript.

5.2. Data Availability Statement

The data presented in this study are available on request from the corresponding author.

5.3. Funding and Acknowledgements

The authors are grateful to Civil Engineering Study Program at Nusa Cendana University, Balai Besar Wilayah Sungai NT II, and several other parties that supported this study.

5.4. Conflicts of Interest

The authors declare no conflict of interest.

6. References

[1] Arifin, Z., Ariantini, M. S., Sudipa, I. G. I., Chaniago, R., Dwipayana, A. D., Adhicandra, I., ... & Alfiah, T. (2023). Green Technology: Application of Environmentally Friendly Technology in Various Fields. Sonpedia Publishing Indonesia, Jambi, Indonesia. (In Indonesian).

[2] BPS-Statistics Indonesia (2024). Kupang Regency Central Statistics Agency, Kupang Regency in Figures 2024. Available online: https://kupangkab.bps.go.id/en/publication/2024/02/28/53d69b4e26e05c2a944307bd/kabupaten-kupang-dalam-angka-2024.html (accessed on May 2025).

[3] PT. Indrakarya (Persero). (2018) Geological and Soil Mechanics Investigation Report, Certification of Design and Test Model of Manikin Dam Kupang (Balai Wilayang Sungai NT II, Kupang, 2018), 47–48.

[4] Manubulu, C. C., Suni, Y. P. K., & Da Costa, D. G. (2023). Determination of River Border Width at the Manikin River in Kupang Regency, Nusa Tenggara Timur Province. IOP Conference Series: Earth and Environmental Science, 1233(1), 012041. doi:10.1088/1755-1315/1233/1/012041.

[5] K Hoeg, K. (1993). Asphaltic concrete cores for embankments dam experience and practise. Norwegian Geotechnical Institute, Oslo, Norway.

[6] Wang, Z., Song, Z., Liu, Y., & Wang, F. (2025). Study on the Seismic Response of an Asphalt Concrete Core Dam-Overburden System Considering the Spatial Variability of Material Parameters. Journal of Earthquake Engineering, 29(2), 525–546. doi:10.1080/13632469.2024.2434518.

[7] Wang, W. (2024). A Material Stress–Strain–Time–Temperature Creep Model for the Analysis of Asphalt Cores in Embankment Dams. Applied Sciences (Switzerland), 14(8). doi:10.3390/app14083399.

[8] Wandira, I. G. P. (2022). Aspal Beton (Asphalt Concrete). NIP. 19660221 199503 1 001. Available online: https://simantu.pu.go.id/personal/img-post/autocover/ad3bf4eb7ddb399c8eb350179e5827c2.pdf (accessed on May 2025).

[9] Smesnik, M., Krstic, S., Guven, S., & Verdianz, M. (2019). Asphalt core embankment dams in turkey–dam design, core material and construction. Proceedings of the ICOLD–European Club Symposium, 2-4 October 2019, Crete, Greece.

[10] Fernández-Gómez, W. D., Rondón Quintana, H., & Reyes Lizcano, F. (2013). A review of asphalt and asphalt mixture aging. Ingenieria e Investigacion, 33(1), 5–12. doi:10.15446/ing.investig.v33n1.37659.

[11] Alicescu, V., Tournier, J. P., & Vannobel, P. (2008). Design and construction of Nemiscau-1 Dam, the first asphalt core rockfill dam in North America. CDA Annual Conference (2008), 27 September-2 October 2008, Winnipeg, Canada.

[12] Wu, S., Pang, L., & Zhu, G. (2008). The effect of ageing on rheological properties and chemical conversions of asphalts. Key Engineering Materials, 385–387, 481–484. doi:10.4028/www.scientific.net/kem.385-387.481.

[13] Zhu, Y., Zhang, Y., Wang, W., & Feng, S. (2023). Could Hydraulic Fracturing Take Place for Asphalt Core in Embankment Dams through Possible Cracks in the Core? Applied Sciences (Switzerland), 13(3), 1523. doi:10.3390/app13031523.

[14] Zhang, H., Yang, X., Li, Y., Fu, Q., & Rui, H. (2022). Laboratory Evaluation of Dynamic Characteristics of a New High-Modulus Asphalt Mixture. Sustainability (Switzerland), 14(19), 11838. doi:10.3390/su141911838.

[15] Zhao, K., Wang, W., Ye, Z., Wang, L., & Liu, C. (2024). Dynamic Response and Fatigue Damage of Asphalt Pavement Under Multiple Coupling Factors. International Journal of Pavement Research and Technology, 17(4), 890–907. doi:10.1007/s42947-023-00275-1.

[16] Restuti, N. A., Juwono, P. T., & Hendrawan, A. P. (2016). Slope Stability Analysis of Wonorejo Dam Based on the 2004 Earthquake Map and the 2010 Earthquake Map. Jurnal Teknik Pengairan: Journal of Water Resources Engineering, 7(1), 73-82. (In Indonesian).

[17] Sugiharti, D., & Susantin, S. H. (2022). Tatic Stability Analysis Of The Cipanas Dam Body, Ujung Jaya District, Sumedang Regency, West Java Province. Prosiding FTSP Series, 31-41 (In Indonesian).

[18] Klau, R. R., Lango, A. K. W., Krisnayanti, D. S., Udiana, I. M., & De Rozari, P. (2024). Prediction of Peak Discharge Using the SCS Curve Number Method in the Manikin Watershed. IOP Conference Series: Earth and Environmental Science, 1343(1), 12007. doi:10.1088/1755-1315/1343/1/012007.

[19] Ananta, M. I., Limantara, L. M., Fidari, J. S., & Nurdin, H. (2024). Design Rainfall Analysis in the Manikin Dam Watershed, Kupang Regency. Jurnal Teknik Sipil, 13(01), 67-78. (In Indonesian).

[20] Krisnayanti, D. S., Welkis, D. F., Sir, T. M. W., Bunganaen, W., & Damayanti, A. C. (2022). Kajian Nilai Curve Number pada Daerah Aliran Sungai Manikin di Kabupaten Kupang. Jurnal Teknik Sumber Daya Air, 1(1), 1–10. doi:10.56860/jtsda.v1i1.3. (In Indonesian).

[21] Damayanti, A. C., Limantara, L. M., & Haribowo, R. (2022). Design Flood Discharge Analysis Using the Nakayasu HSS, ITB-1 HSS, and Limantara HSS Methods in the Manikin Watershed in Kupang Regency. Jurnal Teknologi Dan Rekayasa Sumber Daya Air, 2(2), 313. doi:10.21776/ub.jtresda.2022.002.02.25. (In Indonesian).

[22] Ekasari, S., Halim, A., & Riman, R. (2023). Stability Analysis Study of Dam Body at Banyu Urip Dam using Geostudio 2018 software in Bojonegoro Regency, East Java. Jurnal Teknik Sipil, 30(1), 121–130. doi:10.5614/jts.2023.30.1.14. (In Indonesian).

[23] Alemie, N. A., Wosenie, M. D., Belew, A. Z., Kibret, E. A., & Ayele, W. T. (2021). Performance evaluation of asphalt concrete core earth-rock fill dam relative to clay core earth-rock fill dam in the case of Megech Dam, Ethiopia. Arabian Journal of Geosciences, 14(24), 2712. doi:10.1007/s12517-021-09009-8.

[24] Feng, S., Wang, W., Hu, W., Deng, Y., Yang, J., Wu, S., Zhang, C., & Höeg, K. (2020). Design and performance of the Quxue asphalt-core rockfill dam. Soils and Foundations, 60(4), 1036–1049. doi:10.1016/j.sandf.2020.06.008.

[25] Merga Bayisa, N. (2019). Relative Performance Evaluation of Asphaltic Concrete Core Embankment Dam and Clay Core Embankment Dam: By Plaxis Software Application. American Journal of Science, Engineering and Technology, 4(1), 18. doi:10.11648/j.ajset.20190401.12.

[26] Roy, S., Jain, V.K., Gupta, M., Chitra, R. (2023). Review of Use of Asphaltic Concrete Core in Earthen/Rock Fill Embankment Dam. Earth Retaining Structures and Stability Analysis. IGC 2021, Lecture Notes in Civil Engineering, 303, Springer, Singapore. doi:10.1007/978-981-19-7245-4_29.

[27] Rewtragulpaibul, C., Jaritngam, S., Wannawong, T., & Somchainuek, O. (2024). Design and Construction Practices of Asphalt Core Embankment. International Conference on Road and Airfield Pavement Technology 2023, 1–10. doi:10.1061/9780784485255.001.

[28] Yang, M., Zhong, Q., Hu, L., Li, Y., & Lu, H. (2024). Model tests and numerical simulation of overtopping-induced breach process of the asphalt concrete core dam. Engineering Failure Analysis, 157, 107877. doi:10.1016/j.engfailanal.2023.107877.

[29] Wijaksono, P., & Abdillah, N. (2023). Analysis of the Effect of Adding Asphalt Emulsion on the Shear Strength and CBR Values of Clay Soil. SLUMP TeS: Jurnal Teknik Sipil, 1(2), 101-107. doi:10.35334/be.v1i1.2477. (In Indonesian).

[30] Herz, E., & Vormwald, M. (2007). A material model for creep and fatigue applied to asphalt. Advances in Construction Materials 2007, Springer, Berlin, Germany. doi:10.1007/978-3-540-72448-3_33.

[31] Hussein, M. M., Fattah, M. Y., & Hilal, M. M. (2022). Assessment of Flexible Pavement Behavior under Dynamic Earthquake Loading. Muthanna Journal of Engineering and Technology, 10(1), 1-8. doi:10.52113/3/eng/mjet/2022-10-01/01-08.

[32] Akhtarpour, A., & Khodaii, A. (2012). 2D & 3D nonlinear dynamic analysis of asphaltic concrete core rockfill dam (a Case study). Proceedings of International Symposium on Dams for a changing world, 5 June 2012, Kyoto, Japan.

[33] Tzenkov, A.D., & Schwager, M.V. (2021). Nonlinear FEM Analysis of the Seismic Behavior of the Menta Bituminous-Face Rockfill Dam. Numerical Analysis of Dams, ICOLD-BW 2019. Lecture Notes in Civil Engineering, 91, Springer, Cham, Switzerland. doi:10.1007/978-3-030-51085-5_35.

[34] Li, C., Song, Z., Wang, F., & Liu, Y. (2024). Analysis of the seismic response and failure evaluation of the slabs of asphalt concrete-faced rockfill dams under SV-Waves with arbitrary angles. Computers and Geotechnics, 168, 106125. doi:10.1016/j.compgeo.2024.106125.

[35] Nurtjahjaningtyas, I., Putra, P. P., & Taufiqurohman, S. H. (2021). Risk Factor Classification Effect on Sematok Dam Slopes Stability. Lowland Technology International Journal, 23(1), 9–19.

[36] Pratama, R. R., Suprijanto, H., & Asmaranto, R. (2021). Stability Analysis of the Main Dam Body at Semantok Dam, Nganjuk, East Java.Jurnal Teknologi Dan Rekayasa Sumber Daya Air, 1(1), 89–102. doi:10.21776/ub.jtresda.2021.001.01.08. (In Indonesian).

[37] Makdisi, F. I., & Seed, H. B. (1978). Simplified procedure for estimating dam and embankment earthquake-induced deformations. Journal of the Geotechnical Engineering Division, 104(7), 849-867. doi:10.1061/AJGEB6.0000668.

[38] Kementerian Pekerjaan Umum dan Perumahan Rakyat. (2017). Dam Stability Analysis Module: Slope Stability Calculation. Basic Dam Planning Training. Bandung Kementeri. Pekerj. Umum dan Perumah, Jakarta, Indonesia. (In Indonesian).

[39] BSN. (2016). Static Slope Stability Analysis Method for Embankment Dams. Badan Standardisasi Nasional, Jakarta, Indonesia. (In Indonesian).

[40] Zolkepli, M. F., Ishak, M. F., & Zaini, M. S. I. (2019). Slope stability analysis using modified Fellenius's and Bishop's method. IOP Conference Series: Materials Science and Engineering, 527(1), 12004. doi:10.1088/1757-899X/527/1/012004.

[41] EM 1110-2-1902. (2003). Slope stability. U.S. Army Corps of Engineers, Washington, United States.

[42] Johari, A., Mousavi, S., & Hooshmand Nejad, A. (2015). A seismic slope stability probabilistic model based on Bishop's method using analytical approach. Scientia Iranica, 22(3), 728–741.

[43] Duncan, J. M., Wright, S. G., & Brandon, T. L. (2014). Soil strength and slope stability. John Wiley & Sons, Hoboken, United States.

[44] Suprapto, R. E., Japarussidik, J., Sriyana, S., & Sadono, K. W. (2021). Pelaparado Dam Risk Assessment Based on the Modified ICOLD Method and the Risk Index Method. Teknik, 42(2), 226–235. doi:10.14710/teknik.v42i2.39715. (In Indonesian).

[45] SNI 3432: 2020. (2020). Procedures for Determining Design Flood and Capacity. Badan Standardisasi Nasional, Jakarta, Indonesia. (In Indonesian).

[46] Maretha, L., Darsono, S., & Sadono, K. W. (2020). Stability and Safety Analysis of the Ciawi Dam (dry dam) in West Java Province.Rang Teknik Journal, 3(2), 243-251. doi:10.31869/rtj.v3i2.1793. (In Indonesian).

[47] Bashar, N.A.M., Zainol, M.R.R.M.A., Aziz, M.S.A., Mazlan, A.Z.A., Zawawi, M.H. (2023). Dam Safety: Highlighted Issues and Reliable Assessment for the Sustainable Dam Infrastructure. Proceedings of the 2nd International Conference on Dam Safety Management and Engineering, ICDSME2023 2023, Water Resources Development and Management, Springer, Singapore. doi:10.1007/978-981-99-3708-0_61.

[48] Shafiei, H., & Eskandari, M. S. (2016). A Review of the Embankment Dam with Asphalt Concrete Core. International Journal of Science and Engineering Investigations, 5(54), 111–114.

[49] Noroozi, A. G., Ajalloeian, R., & Bayat, M. (2022). Experimental study of the role of interface element in earth dams with asphalt concrete core - Case study: Mijran dam. Case Studies in Construction Materials, 16. doi:10.1016/j.cscm.2022.e01004.